

## THERMODYNAMIC SIMULATION OF AMMONIA-WATER ABSORPTION REFRIGERATION SYSTEM

by

**A. SATHYABHAMA and T. P. ASHOK BABU**

Original scientific paper  
UDC: 621.5.047:519.876.5:536.24  
BIBLID: 0354-9836, 12 (2008), 3, 45-53  
DOI: 10.2298/TSCI0802045S

*The ammonia-water absorption refrigeration system is attracting increasing research interests, since the system can be powered by waste thermal energy, thus reducing demand on electricity supply. The development of this technology demands reliable and effective system simulations. In this work, a thermodynamic simulation of the cycle is carried out to investigate the effects of different operating variables on the performance of the cycle. A computer program in C language is written for the performance analysis of the cycle.*

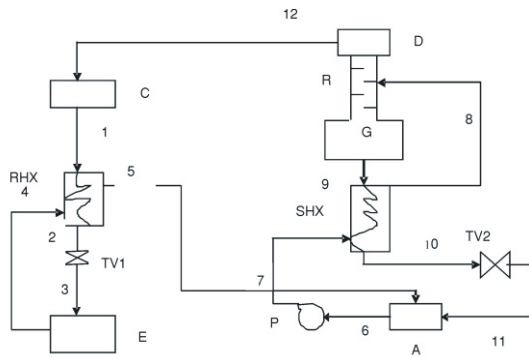
**Key words:** *absorption refrigeration, ammonia-water, computer simulation, operating variables, performance, thermodynamic analysis*

### Introduction

In recent years, theoretical and experimental researches on the absorption refrigeration system (ARS) have increased, because these systems harness inexpensive energy sources (like waste heat from gas and steam turbines, solar, geothermal, biomass) in comparison to vapour compression systems. Besides, ARSs cause no ecological dangers, such as depletion of ozone layer and global warming, and hence they are environment-friendly.

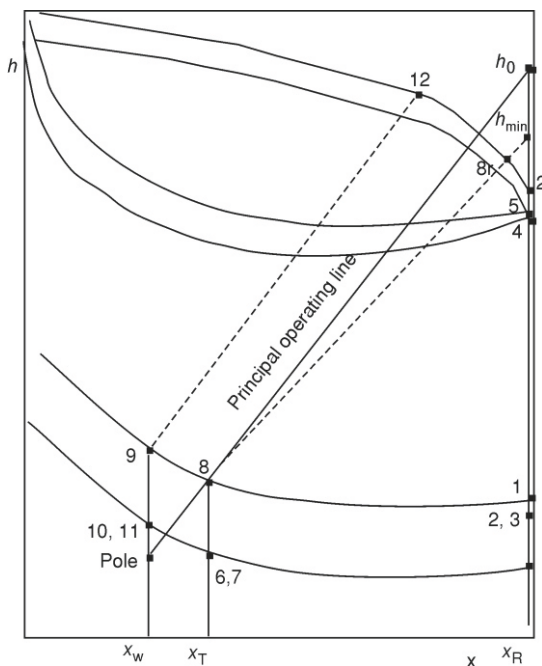
Extensive studies have been reported in literature on the selection of refrigerant absorbent combinations. The combination of ammonia-water has been attractive. Its performance is better than that of fluorocarbon refrigerants used in absorption systems and it is free from the limitations imposed by the high freezing temperature of the refrigerant and low crystallization temperature of the solution, as in water-lithium bromide system, or extreme corrosiveness as in ammonia-sodium thiocyanate system. The only disadvantage of the ammonia-water system is the volatile nature of water used as the absorbent. However this disadvantage can be overcome by incorporating a properly designed rectification column.

Figure 1 sketches the refrigeration system [1]. Evaporator, expansion valve TV1 and condenser operate as in a mechanical compression refrigeration system, with the remaining components playing the role of a compressor. The vapor leaving the evaporator is absorbed by the weak solution in absorber forming the strong solution, which is driven by solution pump to the generator. This is composed of desorber, where ammonia vapor is liberated with a water content still too high for the evaporator, and the components that remove most of the water: distillation/rectification column and dephlegmator. The part of the vapor which is condensed in the dephlegmator returns as reflux (R) to distillation column where it exchanges heat and mass with the ascending vapor. After the dephlegmator, the ammonia vapor is admitted to the condenser.



**Figure 1. Ammonia-water absorption refrigeration system**

*A* – absorber, *R* – rectifying column, *RHX* – refrigerant heat exchanger, *C* – condenser, *D* – dephlegmator, *SHX* – solution heat exchanger, *E* – evaporator, *TV* – throttle valve, *G* – generator, *P* – pump



**Figure 2. *h-x* diagram**

that the refrigerant vapour contains 100% ammonia. Engler *et al.* [8] performed a comprehensive investigation of various ammonia-water cycles, with operating conditions and design parameters varied over a wide range to compare their performance. They employed ABSIM code [9], which were developed specifically for flexible simulation of absorption cycles. Large number of governing equations and the non-linear behavior of the working fluid were solved simultaneously to give the design point performance. ABSIM provides realistic results for the stationary behavior under

The refrigerant heat exchanger (RHX) subcools the liquid refrigerant from the condenser. The solution heat exchanger (SHX) pre-heats the strong solution while pre-cooling the weak solution that leaves the desorber, thus reducing the amount of external heat needed, and also decreasing the required size for both the desorber and the absorber. The various state points are shown in *h-x* diagram in fig. 2.

The development of ammonia absorption refrigeration technology demands reliable and effective system simulations; several computer models have been developed, and have proved to be valuable tools for thermal design optimization. Whitlow [2] has analysed both water cooled and air cooled cycles. Stoecker *et al.* [3] have computed the effects of different operating temperature on *COP* of the cycle. Since no consideration was given to component effectiveness, the calculated *COP* represent the maximum or ideal cycle performance. Shwarts *et al.* [4] analyzed thermodynamically the possibility to operate the solar absorption refrigeration system for air conditioning. Their results showed that the system was suitable for domestic use. Sun [5] analyzed and performed an optimization of the ammonia-water cycle. As a result, he obtained a mathematical model that allowed the simulation of the process. Sun [6] presented a thermodynamic design and performed an optimization of the absorption refrigeration process in order to map the most common cycles for ammonia-water, and water-lithium bromide. The results can be used to select the operation conditions in order to obtain a maximum performance from the system. Sun [7] performed a thermodynamic analysis of different binary mixtures considered in the absorption refrigeration cycle. He assumed

well-defined boundary conditions. Kandlikar [10] has performed a detailed analysis of conventional and modified cycle with absorber heat recovery for ammonia absorption refrigeration system.

### Scope of the present work

Analysis of the absorption cycle is made by several investigators for particular operating conditions and assuming 100% ammonia in the vapour leaving the generator. In this paper complete investigation of the cycle is made by considering the individual component efficiencies.

### Analysis of the cycle

The analysis of the cycle is made under the following assumptions:

- the vapour leaving the dephlegmator is saturated at the average temperature of generator and condenser temperatures,
- the liquid leaving the condenser is saturated at the condenser temperature,
- the strong solution leaving the absorber is saturated at the absorber temperature,
- the weak solution leaving the generator is saturated at the generator temperature,
- the strong solution is heated only up to saturation temperature,
- heat exchanger effectiveness is below 1.0,
- the refrigerant vapour concentration  $x_R$  at the dephlegmator exit is equal to 0.999, and
- condenser and evaporator pressures are condensation and evaporation pressures, respectively; the absorber pressure is equal to evaporator pressure and the generator pressure is similarly equal to the condenser pressure; pressure drops in the system are not taken into consideration.

In this study, the cycle processes were modeled using mass and energy conservation. Equilibrium state thermodynamic properties of ammonia-water solutions required for the analysis are taken from equations developed by Patek *et al.* [11]. These equations were constructed by fitting critically assessed experimental data using simple functional forms. They cover the region within which absorption cycles commonly used operate most often.

Given the generator, condenser, absorber, and evaporator temperatures, and also the cooling load, the state point properties and the quantities of heat supplied and rejected in the different components are calculated as described below:

- the high side and low side pressures are determined from equilibrium correlation:

$$P_h = P(T_c, x_R) \quad (1)$$

$$P_l = P(T_a, x_R) \quad (2)$$

- the strong and the weak solution concentrations are given by:

$$x_s = x(T_a, P_l) \quad (3)$$

$$x_w = x(T_g, P_h) \quad (4)$$

### Condenser, refrigerant heat exchanger and evaporator

Due to imperfect rectification, a small amount of vapour is also carried along with ammonia vapour to the evaporator. The concentration of water in the liquid state increases along

the evaporator as ammonia vaporizes faster, due to which the saturation temperature at the exit of the evaporator is higher than the temperature at the inlet, *i. e.*:

$$T_4 = T_3 + \Delta T_c \quad (5)$$

Temperature of the subcooled refrigerant at state 2:

$$T_2 = T_1 - (T_1 - T_4)E \quad (6)$$

where  $E$  is the effectiveness of RHX.

For throttling process 2-3:

$$h_3 = h_2 \quad (7)$$

The refrigerant flow rate for the given capacity is calculated by a heat balance across the evaporator:

$$m_r = \frac{TOR}{h_4 - h_3} \quad (8)$$

Heat absorbed in the evaporator:

$$Q_e = m_r(h_4 - h_3) \quad (9)$$

Heat rejected in the condenser:

$$Q_c = m_r(h_{12} - h_1) \quad (10)$$

*Absorber, solution heat exchanger, generator*

Enthalpy at state point 7:

$$h_7 = h_6 + (P_h - P_l)v_6 \quad (11)$$

Pump work:

$$W_p = m_s(P_h - P_l)v_6 \quad (12)$$

The mass flow rates of the strong and weak solutions are calculated by making a heat balance over the absorber:

$$m_s = \frac{m_r(x_R - x_w)}{x_s - x_w} \quad (13)$$

$$m_w = m_s - m_r \quad (14)$$

The circulation ratio  $f$  is defined here as the ratio of the mass flow rate of the strong solution entering the generator to the mass flow rate of refrigerant:

$$f = \frac{m_s}{m_r} = \frac{x_R - x_w}{x_s - x_w} \quad (15)$$

Enthalpy at state point 10 is calculated by an energy balance across SHX:

$$h_{10} - h_9 = (h_8 - h_7) \frac{m_s}{m_w} \quad (16)$$

and  $T_{10}$  is now calculated at the known values of  $h_{10}$  and  $x_w$  from:

$$h_{10} = h_1(T_{10}, x_w) \quad (17)$$

For throttling process 10-11:

$$h_{11} = h_{10} \quad (18)$$

Heat rejected in the absorber is calculated by making an energy balance across absorber:

$$Q_a = m_w h_{11} + m_i h_5 - m_s h_6 \quad (19)$$

### Dephlegmator

The extension of the line joining 8 and 8v intersects the line  $x_R$  at  $h_{\min}$ . The enthalpy  $h_{o1}$  can be calculated by the triangle principle, from graphical construction shown in fig. 2

$$h_{\min} - h_8 = \frac{x_R - x_s}{x_{8v} - x_s} (h_{8v} - h_8) \quad (20)$$

But the principal operating line must be steeper than this mixture region isotherm. Hence the operating enthalpy is given by:

$$h_o = h_{12} + [FR_{\min}(h_{\min} - h_{12})] \quad (21)$$

where  $R_{\min}$ , the minimum reflux in the dephlegmator is given by:

$$R_{\min} = \frac{h_{\min} - h_{12}}{h_{12} - h_1} \quad (22)$$

and the reflux ratio  $F$  is defined as the ratio of operating reflux to the minimum reflux.

Heat rejected in the dephlegmator

$$Q_d = m_r (h_o - h_{12}) \quad (23)$$

Then enthalpy  $h_p$  is given by the triangle principle, from the graphical construction in fig. 2:

$$h_p - h_o = \frac{x_R - x_w}{x_R - x_s} (h_o - h_s) \quad (24)$$

Heat input to the generator:

$$Q_g = m_w (h_9 - h_p) \quad (25)$$

$$COP = \frac{Q_c - W_p}{Q_g} \quad (26)$$

Finally energy balance yields:

$$Q_g + Q_c + W_p = Q_c + Q_a + Q_d + \text{error} \quad (27)$$

A computer program in C language is written for the above analysis.

### Description of the program

The program is constructed to allow for a sequential computation of more than one problem. For each problem, the user provides the following information:

- capacity of the system,
- generator temperature,

- condenser temperature,
- evaporator temperature, and
- absorber temperature.

The main program calls on subroutines for the thermodynamic properties of the ammonia-water mixture at different states. For the calculation of thermodynamic properties, both in vapour and liquid phases as well as the vapour-liquid equilibrium, the simplified formulation proposed by Patek *et al.* [10] are used in this work. These equations are in the following form:

$$T_x = F_1(p, x)$$

$$T_y = F_1(p, y)$$

$$y = F_2(p, x)$$

$$h_1 = F_3(T, x)$$

$$h_v = F_4(T, y)$$

For calculating any property on right hand side of the above equations, for example, to calculate  $T$  when  $h_1$  and  $x$  are given, an iterative scheme using Newton-Raphson method is used. The main program then calculates the heat rejected/absorbed in various components of the cycle like the condenser, evaporator, absorber, dephlegmator, pump, generator, and the  $COP$  of the cycle. The results along with input data are then printed in a file named “output”.

## Results and discussions

Output of the program for one set of operating conditions are shown below.

### Input data

– capacity	1.0 TOR
– generator temperature	373.00 K
– condenser temperature	303.00 K
– absorber temperature	303.00 K
– evaporator temperature	268.00 K
– vapour concentration after dephlegmator	0.9990

### Results

– condenser pressure	1.1720 MPa
– evaporator pressure	0.3581 MPa
– weak solution concentration	0.3495
– rich solution concentration	0.5049
– vapour concentration after generator	0.9859
– mass flow of refrigerant	0.00279 kg/s
– rich solution flowrate	0.01167 kg/s
– weak solution flowrate	0.00888 kg/s
– circulation ratio	0.761
– heat input to the generator $Q_g$	5.301 kJ
– heat rejected in the absorber $Q_a$	5.100 kJ
– heat rejected in the condenser $Q_c$	3.328 kJ
– heat absorbed in the evaporator $Q_e$	3.500 kJ
– heat rejected in the dephlegmator $Q_d$	0.408 kJ

- pump work  $W_p$  0.035 kJ
- $COP$  0.656

In order to find the performance of the system under different operating conditions following range of operating conditions are used:

- generator temperature from 60 to 140 °C,
- condenser and absorber temperature from 30 to 50 °C,
- evaporator temperature from -5 to +5 °C, and
- with heat exchanger efficiency of 80%.

The variation of  $COP$  with generator temperature is shown in fig. 3 for three values of condenser and absorber temperature. Increase in condenser and absorber temperature decreases the system performance.  $COP$ , in general increases with generator temperature reaches a maximum and then decreases as a result of increase in irreversibility at higher generator temperature. For condenser and absorber temperature of 25 °C, the maximum  $COP$  is 0.75 and occurs at generator temperature of 65 °C. For condenser temperature of 30 °C, maximum  $COP$  is 0.67 and occurs at generator temperature of 77 °C. Maximum  $COP$  is 0.57 at generator temperature of 97 °C, for condenser temperature of 40 °C. There is a minimum generator temperature for each set of specified operation conditions below which the system cannot function.

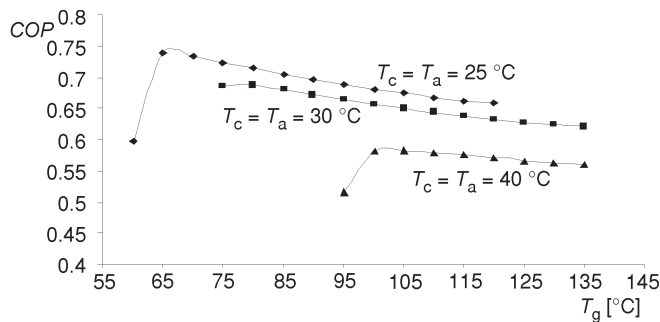


Figure 3. Effect of generator temperature on  $COP$

Figure 4 shows the variation of circulation ratio with generator temperature. At lower generator temperature the difference between rich and weak solution concentration is small resulting in higher circulation ratio as per eq. (15). This means that the solution pump has to run faster or a bigger pump is required. At a given generator pressure, weak solution concentration ( $x_w$ ) is determined by generator temperature. If the generator temperature reaches its lower limit, the circulation ratio increases dramatically making the system inefficient. Also circulation ratio is lower for low condenser temperature due to higher  $x_s$  values. Figure 5 shows the variation of  $COP$  with evaporator temperature for different values of generator and condenser temperatures.

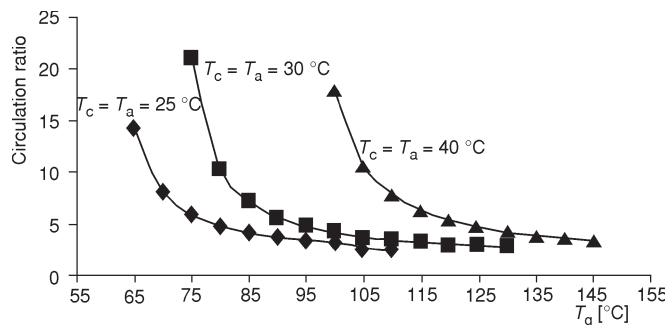


Figure 4. Effect of generator temperature on circulation ratio

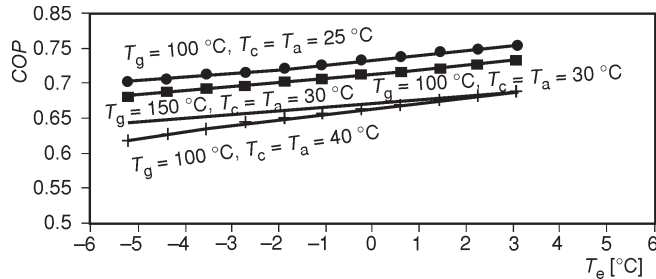


Figure 5. Effect of evaporator temperature on *COP*

*COP* increases with increase in evaporator temperature and higher *COP* is obtained for lower condenser and absorber temperature at constant generator temperature. At constant condenser and absorber temperature, *COP* is higher at lower generator temperature. Figure 6 shows the variation of *COP* with condenser and absorber temperature for generator temperature 100 °C. It is observed that variation of *COP* with absorber temperature is more prominent than with condenser temperature. Same pattern is observed at generator temperature 150 °C (fig. 7).

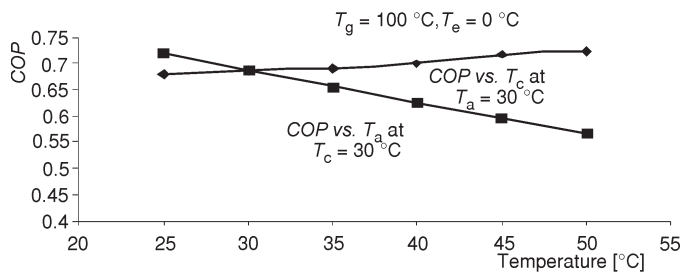


Figure 6. Effect of condenser and absorber Temperature on *COP* at  $T_g = 100\text{ }^\circ\text{C}$

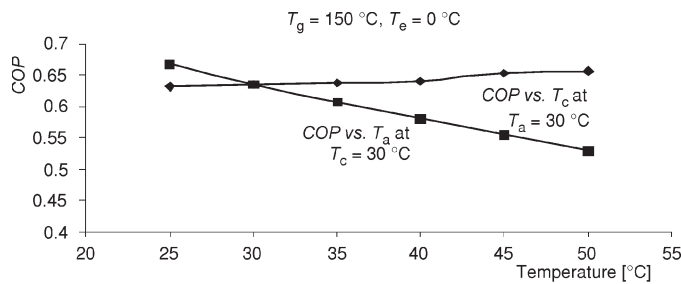


Figure 7. Effect of condenser and absorber Temperature on *COP* at  $T_g = 150\text{ }^\circ\text{C}$

## Conclusions

A computer simulation is done to study the effect of operating variables on the performance of ammonia-water absorption refrigeration system with their thermodynamic properties expressed in polynomial equations. The simulation is carried out for specific operating temperatures. From the results it is observed that we cannot choose an arbitrary combination of operating temperatures. For condenser and absorber temperature of 25 °C, the maximum *COP* is 0.75 and occurs at generator temperature of 65 °C. For condenser temperature of 30 °C, maximum *COP* is 0.67 and occurs at generator temperature of 77 °C. Maximum *COP* is 0.57 at generator temperature of 97 °C, for condenser temperature of 40 °C. One has to be careful in selecting the operating variables as low heat rejection or high generator temperature, do not necessarily give higher *COP* values.



## Nomenclature

<i>COP</i>	– coefficient of performance, [–]
<i>E</i>	– effectiveness of heat exchanger, [–]
<i>F</i>	– reflux ratio, [–]
<i>f</i>	– circulation ratio
<i>h</i>	– enthalpy [ $\text{kJkg}^{-1}\text{K}^{-1}$ ]
<i>m</i>	– mass flow rate [ $\text{kgs}^{-1}$ ]
<i>P</i>	– pressure, [bar]
<i>Q</i>	– heat quantity, [kW]
<i>R</i>	– reflux
<i>T</i>	– temperature, [K]
<i>TOR</i>	– tons of refrigeration, [t]
<i>v</i>	– specific volume, [ $\text{m}^3\text{kg}^{-1}\text{s}^{-1}$ ]
<i>W</i>	– work quantity, [kW]
<i>x</i>	– ammonia mole fraction in liquid phase
<i>y</i>	– ammonia mole fraction in vapour phase, [–]

## Subscripts

a	– absorber
c	– condenser
d	– dephlegmator
e	– evaporator
g	– generator
l	– liquid phase of water-ammonia mixture
min	– minimum
o	– operating
p	– pole
r	– refrigerant
s	– strong ammonia solution
v	– vapour phase of water-ammonia mixture
w	– weak ammonia solution

## References

- [1] Threlkeld, J. L., Thermal Environmental Engineering, Prentice Hall, Upper Sadle River, N. J., USA, 1962
- [2] Whitlow, E. P., Trends of Efficiencies in Absorption Refrigeration Machines, *ASHRAE Journal*, 8 (1966), 13, pp. 44-48
- [3] Stoecker, W. F., Reed, L. D., Effect of Operating Temperatures on the Coefficient of Performance of Aqua-Ammonia Refrigerating Systems, *ASHRAE Transactions*, 77 (1971), 1, pp. 163-173
- [4] Shwartz, I., Shitzer, A., Solar Absorption System for Space Cooling and Heating, *ASHRAE Journal*, 19 (1977), 11, pp. 51-54
- [5] Sun, D. W., Computer Simulation and Optimization of Ammonia-Water Absorption Refrigeration Systems, *Energy Sources*, 17 (1976), 3, pp. 211-221
- [6] Sun, D. W., Thermodynamic Design Data and Optimum Design Maps for Absorption Refrigeration Systems, *Applied Thermal Engineering*, 17 (1997), 3, pp. 211-221
- [7] Sun, D. W., Comparison of the Performances of  $\text{NH}_3\text{-H}_2\text{O}$ ,  $\text{NH}_3\text{-LiNO}_3$  and  $\text{NH}_3\text{-NaSCN}$  Absorption Refrigeration Systems, *Energy Conversion Management*, 39 (1998), 5/6, pp. 357-368
- [8] Engler, M., Grossman, G., Hellmann, H. M., Comparative Simulation and Investigation of Ammonia/Water Absorption Cycles for Heat Pump Applications, *Int. J. Refrigeration* 20 (1997), 7, pp. 504-516
- [9] Grossman, G., Wilk, M., Advanced Modular Simulation of Absorption Systems, *Int. J. Refrigeration*, 17 (1994), 4, pp. 231-244
- [10] Kandlikar, S. G., A New Absorber Heat Recovery Cycle to Improve COP of Aqua Ammonia Absorption Refrigeration System, *ASHRAE Transactions*, 88 (1982), 1, pp. 141-158
- [11] Patek, J., Klomfar, J., Simple Functions for Fast Calculations of Selected Thermodynamic Properties of the Ammonia-Water System, *Int. J. Refrigeration*, 18 (1995), 4, pp. 228-234

Authors' address:

A. Sathyabhama T. P. Ashok Babu  
 Dept. of Mech. Engg., National Institute of Technology Karnataka  
 Surathkal Post Srinivasnagar,  
 Mangalore – 575 025, Karnataka, India

Corresponding author A. Sathyabhama  
 E-mail: sathyabhamaa@hotmail.com

Paper submitted: November 3, 2007  
 Paper revised: March 25, 2008  
 Paper accepted: April 10, 2008